Evaluation of Genetic Algorithms in Mitigating Wireless Interference in Situ at 2.4 GHz

Jonathan Becker and Jason Lohn
Carnegie Mellon University
Pittsburgh, PA, USA

Derek Linden
X5 Systems Inc.
Ashburn, VA USA

***Abstract*—This paper compares the Simple Genetic Algorithm (SGA) to the Triallelic Diploid Genetic Algorithm (TDGA) in evolving an anti-jamming beamforming array in situ. The SGA and TDGA are both able to find reasonable beamformer settings that thwart two stationary interferers while allowing reception of a stationary signal of interest (SOI). We evaluate the TDGA's performance in thwarting mobile interferers with stationary and mobile SOIs. The array operates in the 2.4 GHz 802.11g WiFi band, and the results presented are applicable to other applications because the SGA and TGDA do not require signal directions and modulation schemes a priori. Analysis of SGA and TDGA convergence times is also presented.**

***Index Terms*—Adaptive arrays, phased arrays, genetic algorithms, anti-jamming, wireless networks, evolved hardware.**

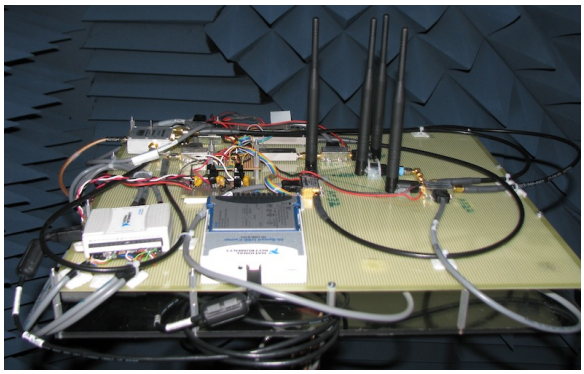

Fig. 1. Beamforming antenna array in anechoic chamber.

I. Introduction

This paper compares the Simple Genetic Algorithm (SGA) to a Triallelic Diploid Genetic Algorithm (TDGA) in evolving a four-antenna anti-jamming beamforming array in situ. The array operates in the 802.11b/g WiFi 2.4 GHz frequency band. The SGA and TDGA optimize a four-antenna beamforming array for mitigating interferers in indoor WiFi communications where multiple interferers (i.e., jammers) prevent communication between a WiFi base station and a WiFi receiver.

A beamforming array focuses electromagnetic (EM) energy on a signal of interest (SOI) while simultaneously minimizing EM energy in interferer directions. We assume that the jammers and SOI directions of arrivals (DOAs) are not known a priori. This problem is difficult in that the solution search space is on the order of trillions and would require thousands of years to solve using a brute force approach. Beamforming arrays typically use dozens to hundreds of antennas and are impractical for non-military applications [1], [2]. To the best of our knowledge, the problem of optimizing a four-antenna beamforming array has not been solved by other groups, so this is a novel solution to a difficult problem.

Lee [3] noted that interference problems between femtocell base stations occur because many such base stations are installed in confined areas. It was shown in simulations that interference could be mitigated through a combination of coordinated user scheduling (CUS) and two beamforming techniques. Because WiFi base stations are typically installed indoors, they could be considered femtocells. CUS is infeasible because jammers may not be WiFi devices. Our method inherently includes channel properties in EM measurements.

Previously, Massa [4] simulated an SGA with real-time parameterized crossover and mutation probabilities to thwart interferers having randomly varying DOAs. The crossover and mutation probabilities were parameterized based on the variance of the binary strings in a population of N trial solutions. These probabilities varied linearly with variance with crossover and probability mutation probabilities maximized with low variance. The modified SGA also discarded a percentage of δ(k) solutions at the k^{th} iteration that are replaced with randomly generated strings.

Weile [5] simulated a GA that used dominance and diploidy to null out five mobile jammers with an a 20 antenna array. It was noted that the SGA's convergence "renders the crossover useless. Thus, if the interference impinging on the array changes, the GA can adapt only through the action of the mutation operator – that is, by a painful process of blind guesswork" [5]. To thwart mobile jammers, Weile used a dominance and diploidy Genetic Algorithm (D&DGA) with triallelic diploid strings based on the theory developed by Goldberg [6]. Weile showed that the D&DGA thwarted mobile jammer sets that changed every 20 generations, and the SGA could not adapt to the second jammer set as expected. The D&DGA also successfully thwarted jammer sets that changed between three different subset [5].

The TDGA presented in this paper is of the same form discussed in detail by Weile [5] and Goldberg [6], and it is implemented in hardware. We presented the TDGA briefly in [7], and it successfully nulled two mobile jammers regardless if the SOI was mobile or stationary. The beamforming array

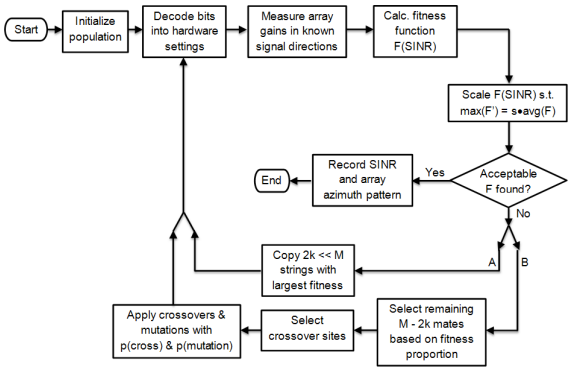

Fig. 2. Block diagram of Genetic Algorithm.

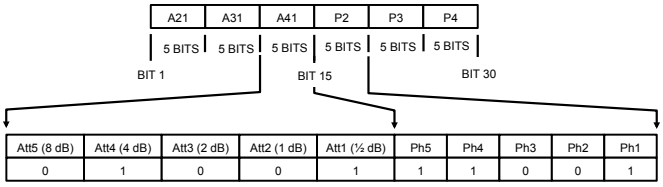

Fig. 3. GA string hardware settings encoding with example encoding.

achieved null depths of 20 dB (with respect to the SOI) which was significantly better than our prior work [2].

We further analyze and compare the SGA and TDGA performance against stationary signals and mobile signals. We present the beamforming array with two jammers and one SOI. The remainder of this paper is as follows. Section II describes the experimental setup and analyzes the results. Section III discusses our conclusions.

II. Experimental Setup and Results

The beamforming array was described in [7]. Previous simulations by Lohn assumed that the antenna elements were infinitesimal dipoles, and the array gain patterns were calculated using the array factor equation [1]. They do not include EM coupling between antennas and reflections off hardware. Antenna coupling could be easily accounted for in simulation tools such as Numerical Electromagnetics Code (NEC) and High Frequency Structure Simulator (HFSS). The hardware components would be time-consuming to model and simulate with those tools. The simulations tools also cannot account for non-linearities such as control-voltage dependent phase-shifter losses. Thus, a practical advantage of this hardware-in-the-loop system is that it overcomes these problems.

The block diagram of a genetic algorithm (GA) is shown in Fig. 2. The SGA and TGDA operate on a population of 30 bit binary strings that encode the antenna phase and attenuation settings for the beamforming array as described in [2]. The first 15 bits represent the settings for the three step-attenuators, as each step-attenuator is controlled by five bits. The remaining 15 bits represent the settings for the three phase shifters. Each phase shifter uses five bits which encodes to 11.6°per bit, as the phase shifters have ±5°tolerance. Fig. 3 shows how the GA encodes the 30 bit string into hardware settings for the three step-attenuators and phase shifters. The example encoding shows the first step attenuator in antenna path four set to 4.5 dB and the phase shifter in path two set to 151°. Table I lists common parameters used in the SGA and TDGA.

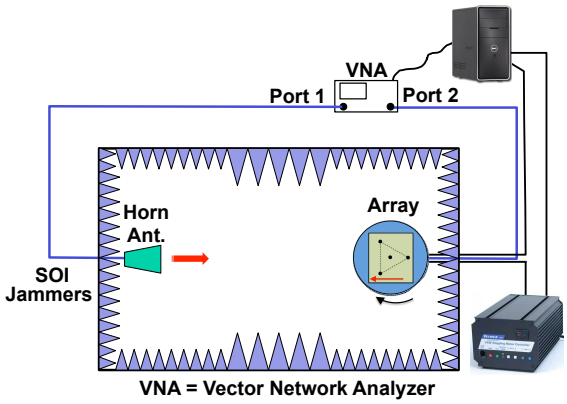

Fig. 4. Experimental test setup with array inside an anechoic chamber.

TABLE I
Parameters Used in GA Optimization Experiments

Parameter	Value(s)
Probablily of Crossover, $\mathbf{P_c}$	0.6
Probability of Mutation, $\mathbf{P_m}$	0.02 1st5 generations 0.01 otherwise
Number of Elite Strings, $\mathbf{n_e}$	4
Population Size, **M**	100, 200

The TDGA performs a two-step crossover as described by Weile and Goldberg [5], [6]. After the TDGA selected a pair of mates, crossover is performed between the upper and lower strings of each diploid individual. This forms a pair of gametes. The upper and lower gametes of the first individual are swapped with the lower and upper gametes of the second individual. The two hybridized children are then expressed as a single child through a process of triallelic dominance where a negative one valued allele represents a recessive one, and a positive one represents a dominant one. A zero valued allele is always recessive. This value will be expressed at a bit location if both children have zero valued alleles or if one child has a recessive one and a zero. If a child has a dominant one, a one valued allele will always be expressed regardless of the other bit value. Mutation is performed after this two-step crossover in the same fashion as the SGA.

Fig. 4 shows the experimental test setup. The beamforming array is mounted in the anechoic chamber on a Delrin pipe attached to a stepper motor on a turntable. Each step is 1/40th of a degree. The source antenna is a wideband 0.3 GHz to 3.0 GHz horn antenna on a mount that allows it to be rotated for either horizontal or vertical polarization. The beamforming array is rotated in 5°steps when an azimuth radiation pattern is measured, and each azimuth pattern measurement takes roughly 10 minutes. For details on the GA interface, see [7].

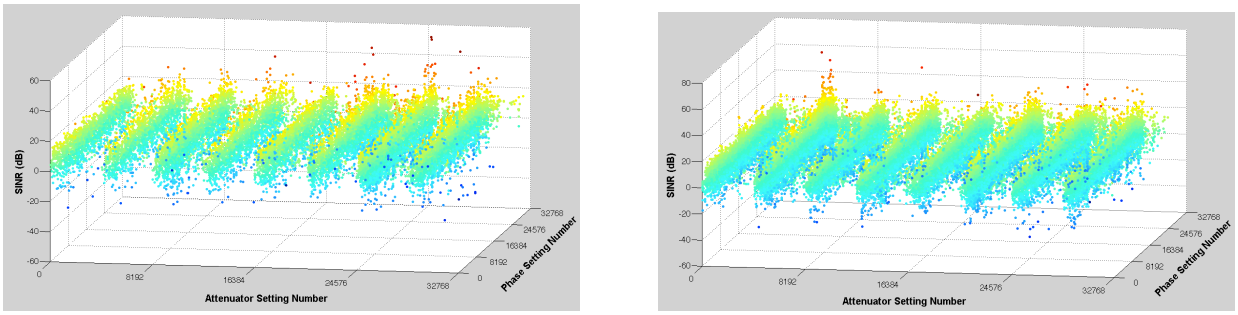

(a) (b)

Fig. 5. SGA SINR Landscape for SOI = 0°and Jammers = [45°, 200°]: (a) M = 100 strings, (b) M = 200 strings

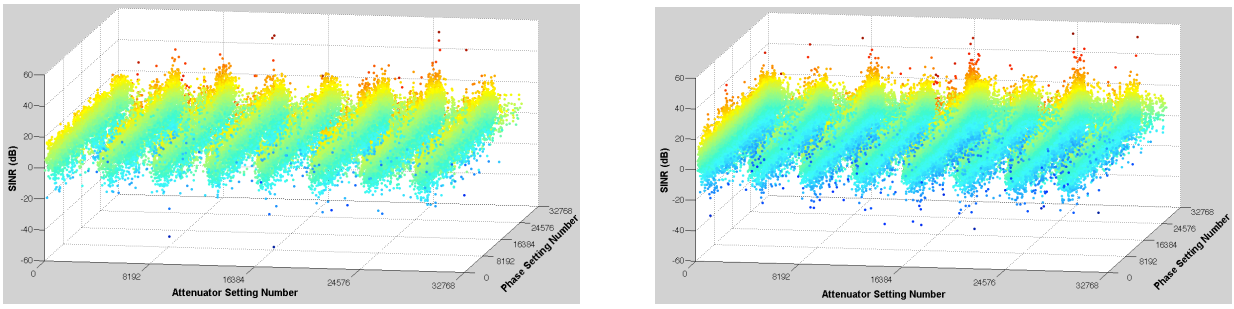

(a) (b)

Fig. 6. TDGA SINR Landscape for SOI = 0°and Jammers = [45°, 200°]: (a) M = 100 strings, (b) M = 200 strings

A. SINR Fitness Landscape for Stationary Signals

In this section, we show that the fitness landscape is highly multimodal when the beamforming array thwarts two jammers and focuses RF energy on a single SOI. To create a fitness landscape, we split the binary encoding string in half as shown in Fig. 3 and convert the two 15-bit binary numbers into decimal formats. The first 15-bit binary to decimal conversion creates a number x that represents the settings for the three step-attenuators and has values $0 \leq x \leq 2^{15} - 1 = 32767$. The second binary to decimal conversion creates a number y that represents the three phase shifter settings and has values $0 \leq y \leq 2^{15} - 1 = 32767$.

As shown in [2], the SINR fitness landscape for the three jammer and one SOI case was highly multimodal. Figs. 5 and 6 show that this is still the case when the DOA for the SOI is 0°and the DOAs for the jammers are 45°and 200°. The landscapes in Fig. 5 represent the landscape that the SGA with M = [100, 200] strings found during its searches to maximize SINR. Fig. 6 shows the M = [100, 200] TDGA landscapes.

It should be noted that the landscapes are based on the locations where the SGA and TGDA focused their searches and are therefore approximations of the actual SINR landscapes. Figs. 5 and 6 clearly show that the SINR fitness landscape is multimodal and is therefore a difficult problem for the SGA and TDGA to solve. The SGA with a population of 100 strings focused its search more erratically around peaks throughout $0 \leq x \leq 32767$ and $24576 \leq y \leq 32767$, as it found many points with $SINR \geq 20dB$ within that range. The SGA with a 200 strings population was less erratic in comparison.

The TDGA's fitness landscape in Fig. 6 differs from Fig. 5 in a subtle manner. The M = 200 string TDGA fitness landscape is more erratic than the 100 string population. The M = 200 string TDGA found more solutions with $SINR \geq 20dB$ in the range $0 \leq x \leq 32767$ and $24576 \leq y \leq 32767$ than the 100 string population. This is an indication that the TDGA is better equipped to handle a multimodal fitness function than the SGA in solving the beamforming problem. We provide additional analysis in the next section.

B. SGA & TDGA Applied to Stationary Signals

Fig. 7 shows the SINR of the fittest string averaged over all runs of the SGA and TDGA for M = [100, 200] strings. The error bars represent ± 1 standard deviation in dB. Because the error bars overlap in the four cases, the means for these four cases are statistically equivalent. However, the M = 200 strings TDGA has the smallest standard deviation out of the four cases. This indicates that the TDGA is better suited than the SGA for solving this problem. The standard deviation for the M = 200 strings SGA shown in Fig. 7b is similar in size to the 100 string population of the SGA shown in Fig. 7a.

To show that there is statistical significance between the SGA and TDGA in solving the beamforming problem for stationary signals, we calculate the confidence coefficient $(1-\alpha)$ for a ± 3 dB confidence interval surrounding the mean of best SINR found for the four GA cases shown in Fig. 7. According to Papoulis [8], the confidence coefficient estimate for a given confidence interval can be calculated under the

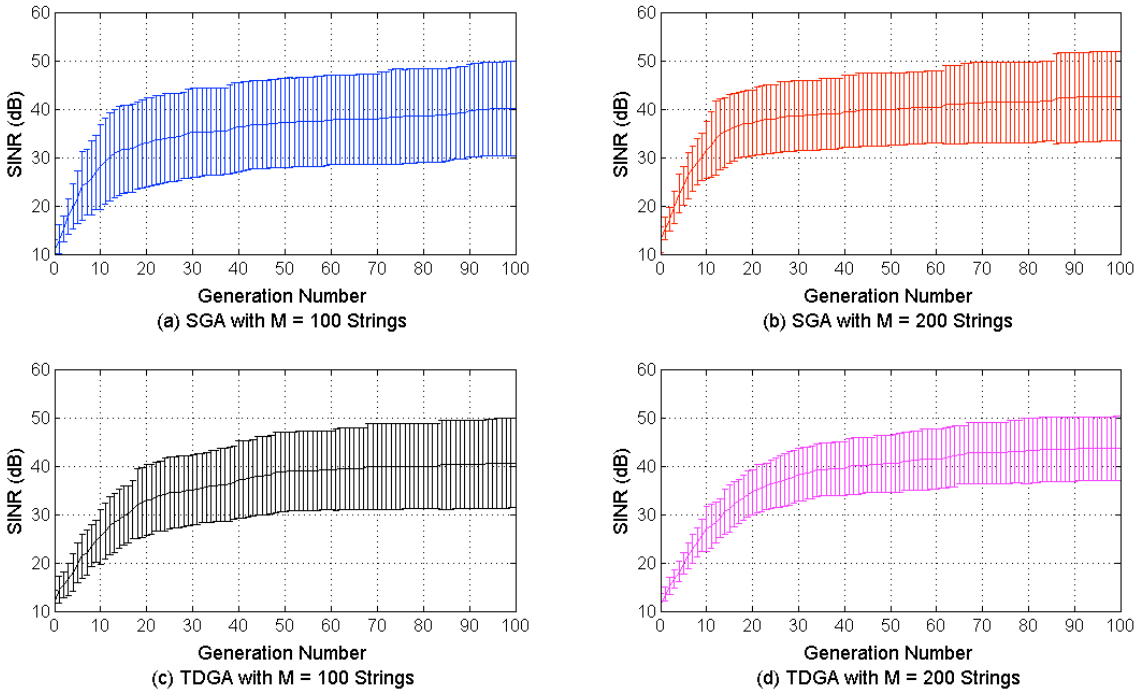

Fig. 7. SINR (dB) of the best (i.e., fittest) string in each population vs. generation number averaged over all runs of the SGA and TDGA for SOI = 0°and Jammers = [45°, 200°]. The error bars are ±1 standard deviation in dB. 30 independent runs were used for each of the four cases shown here.

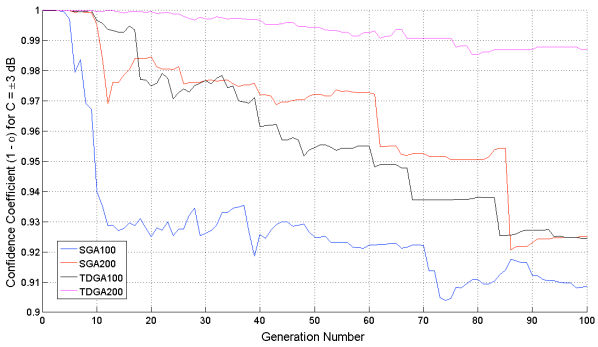

Fig. 8. Confidence Coefficients for the SGA and TDGA with C = ± 3 dB

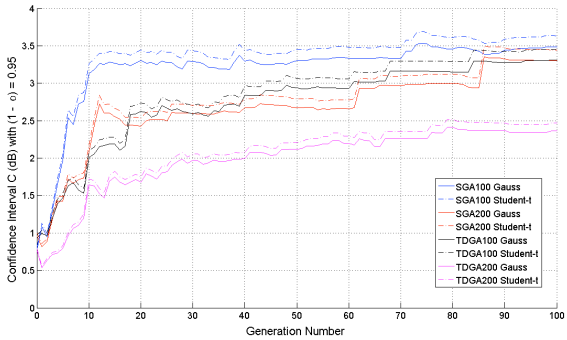

Fig. 9. Confidence intervals ±C dB with 95% confidence coefficient

assumption that the processes are independent and identically distributed (i.i.d.) Gaussian using equation (1):

$$P\{SINR_{Best}(K,n) - C \leq SINR_{Best,Mean}(K,n) \leq SINR_{Best}(K,n) + C\} > 1 - \alpha \quad (1)$$

where

$$1 - \alpha = 1 - 2Q(c\sqrt{(K)}/\sigma_{SINR(K,n)}) \quad (2)$$

and $0 \leq n \leq N = 100$ is the generation number. Each run of the SGA and TDGA are i.i.d. because we seed the random number generator (RNG) that creates the initial populations with a different prime integer at the start of each run, and the beamforming array is tested inside a controlled environment. Because the number of runs K = 30, and each run of the GAs is i.i.d., the Central Limit Theorem applies, and the results produced by the SGA and TDGA are Gaussian [8].

Fig. 8 shows the results of our confidence coefficient calculations for the SGA and TDGAs with populations $M = 100, 200$ strings. The ±3 dB case is important, as it indicates the likelihood that the best solutions found in any generation by the SGA and TDGA are within a half to double power margin surrounding the mean of the best solutions.

Both the SGA and TDGA had 100% confidence coefficients initially. The initial populations were chosen at random and had low SINRs. The $M = 100$ strings population SGA confidence coefficient approached 90% as it evolved, and the SGA with $M = 200$ strings faired slightly better having approached a confidence coefficient of 92.1% at generation 87 and a final confidence coefficient of 92.5% at generation

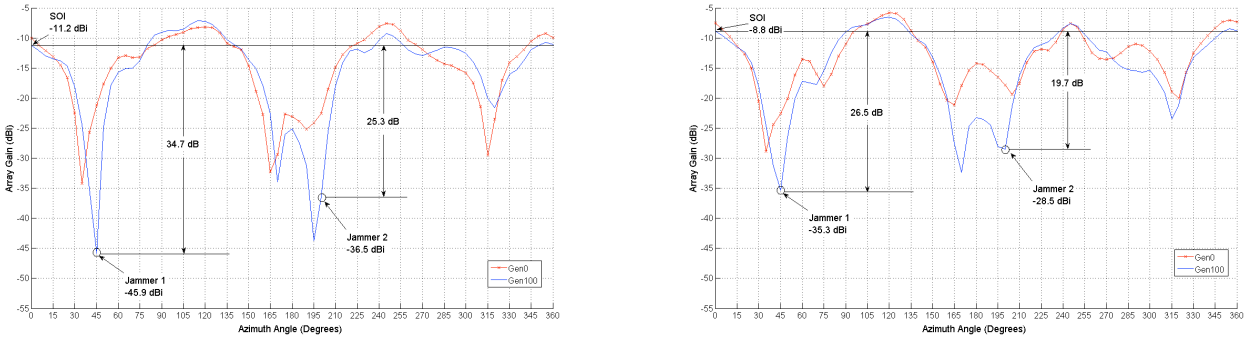

(a) (b)

Fig. 10. Azimuth radiation plots with $M = 100$ strings SGA having stationary signals for the best and worst cases of the fittest solutions found by the SGA in independent 30 runs. SOI = 0°and Jammers = [45°, 200°]: (a) Best fittest solution found in Run 7, (b) Worst fittest solution found in Run 30

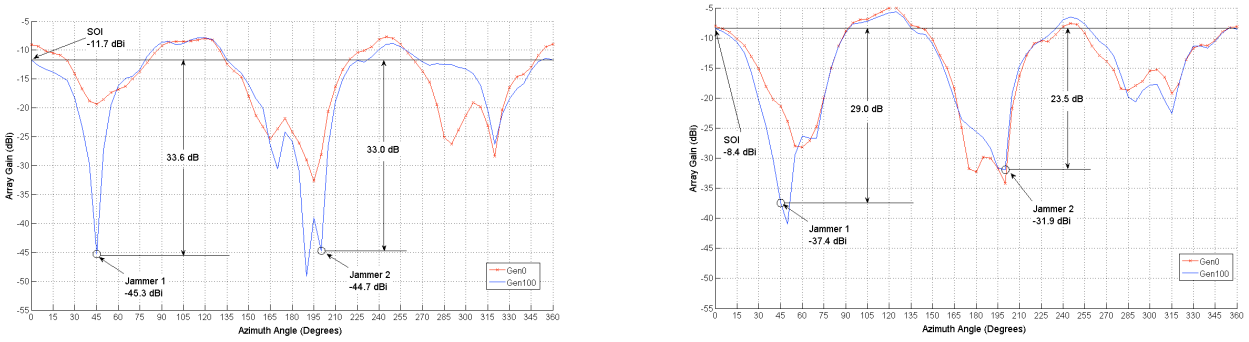

(a) (b)

Fig. 11. Azimuth radiation plots with $M = 200$ strings SGA having stationary signals for the best and worst cases of the fittest solutions found by the SGA in independent 30 runs. SOI = 0°and Jammers = [45°, 200°]: (a) Best fittest solution found in Run 24, (b) Worst fittest solution found in Run 30

100. The SGA's confidence coefficient decreased as the SGA created better solutions because the SGA tends to lose bitwise information as it created strings with higher fitness [9].

The $M = 100$ strings TDGA had a minimum confidence coefficient of 92.4% at generation 100. This is roughly the same as the $M = 200$ population SGA. The $M = 200$ strings TDGA had a minimum confidence coefficient of 98.5% at generation 81 and a final confidence coefficient of 98.7% at generation 100. These results indicated that the TDGA is better equipped to solve the beamforming with stationary signals problem than the SGA. This is expected, as Weile et. al. [5] and Goldberg [6] both noted that diploid strings store long-term memory beyond the previous $n-1$ generation. The TDGA is better able to retain bitwise information that would otherwise be lost during the mate selection process.

We verified our results in Fig. 8 by plotting confidence intervals ($\pm$ C dB) of the M = [100, 200] SGA and TDGA cases for a 95% confidence coefficient. Fig. 9 shows confidence intervals calculated assuming a Gaussian distribution and confidence intervals based on a Student-t distribution. The Gaussian and Student-t confidence interval calculations are nearly identical with a constant 4.2% error. This is expected since the Student-t distribution approaches a normal distribution for $K \geq 30$ [8]. The M = 200 TDGA performed best with final 2.4 dB Gaussian & 2.5 dB Student-t confidence intervals.

Figs. 10 - 13 show the Azimuth radiation plots for the best and worst cases of the fittest solutions found by the SGA and TDGA. Data was collected from 30 independent runs each for the SGA and TDGA with populations of $M = 100$ strings and $M = 200$ strings. The signals are stationary with directions of arrival(DOA) for the SOI = 0°and jammers = [45°, 200°].

The generation 100 Azimuth plots shown Fig. 10a and Fig. 10b correspond to SINR fitness values of 55.5 dB and 24.1 dB respectively. The generation 100 plots shows in Fig. 11a and Fig. 11b correspond to SINR fitness values of 67.8 dB and 28.3 dB. These fitness values were recorded by the SGA when it computed and compared string fitness values. The motor did not move while the SGA computed all fitness values in each generation, and the motor rotated in the directions of the SOI and jammer before the SGA took M = [100, 200] measurements at those angles. However, the motor was rotated from 0°to 360°(in 5°steps) to measure Azimuth radiation patterns. Although the VNA averaged measurements, variations due to motor movements limited the null depths seen

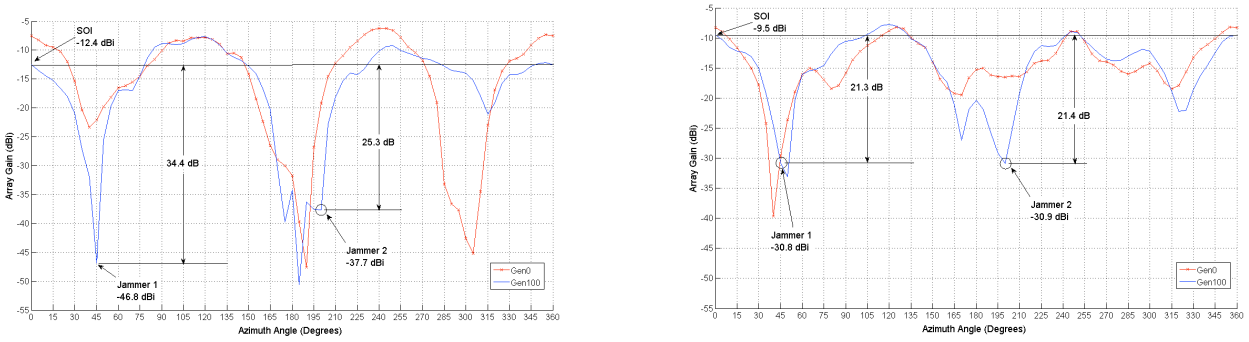

(a) (b)

Fig. 12. Azimuth radiation plots with $M = 100$ strings TDGA having stationary signals for the best and worst cases of the fittest solutions found by the SGA in independent 30 runs. SOI = 0°and Jammers = [45°, 200°]: (a) Best fittest solution found in Run 20, (b) Worst fittest solution found in Run 10

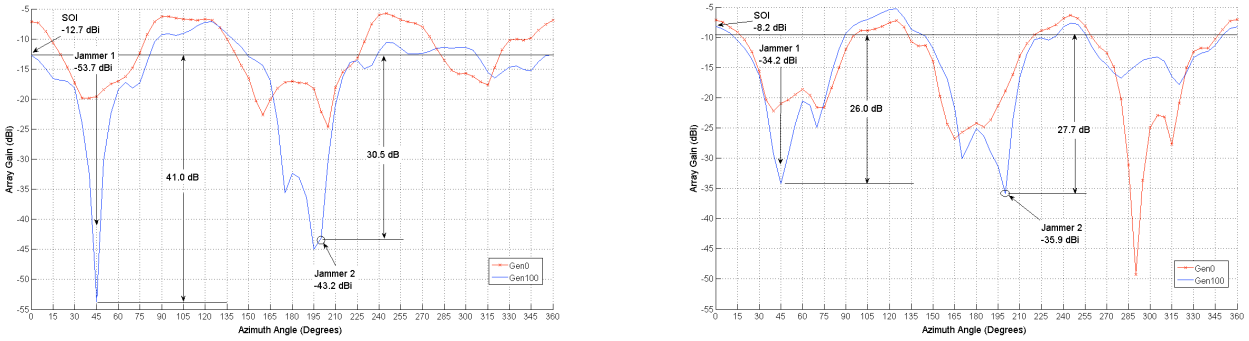

(a) (b)

Fig. 13. Azimuth radiation plots with $M = 200$ strings TDGA having stationary signals for the best and worst cases of the fittest solutions found by the SGA in independent 30 runs. SOI = 0°and Jammers = [45°, 200°]: (a) Best fittest solution found in Run 3, (b) Worst fittest solution found in Run 29

in these plots. It was not feasible to pause the motor for more than a few seconds after each rotation. This would cause each Azimuth pattern measurement to take over 30 minutes. With error due to motor movement considered, the shallowest null depth between SOI and interferers was 19.7 dB.

Fig. 12a and Fig. 12b show the Azimuth plots associated with best and worst cases of the fittest solutions that the TDGA found for stationary signals with this set of stationary SOI and jammers and a population of 100 strings. The worst and best of the fittest solutions measured by the TDGA had SINRs of 56.6 dB and 21.1 dB respectively. In addition, the Azimuth plots shown in Fig. 13a and Fig. 13b correspond to best and worst case values of fittest solutions having 55.5 dB and 31.1 dB. The TDGA had a population of 200 strings.

The Azimuth plots in conjunction with Fig. 7 show that the SGA and TDGA both have a large variation in the final SINR values that both algorithm variants found. However, both the SGA and TDGA found acceptable solutions even in the worst case. We will focus on improving the TDGA and explore other algorithms in future works. It is believed that the SGA cannot handle mobile jammers, as the mating process tends to select the best few solutions and fill future populations with copies of those solutions. This renders the crossover operator useless because the bits swapped between mated pairs of strings are the same. Information that present in the initial population and not relevant to the current fitness landscape was lost. Although the mutation operator can recover a small portion of this information, the recovery isn't at a rate sufficient for the SGA to adapt to a changing fitness function ([6], [9]). Our own unpublished simulations showed that the SGA cannot readapt to another solution if the signal directions are changed after the SGA has converged to a good solution. In the next section, we show that the TDGA can thwart mobile interferers both when the SOI is stationary and mobile.

C. Performance of TDGA Adapting to Mobile Signals

Weile's simulations showed that triallelic encoded diploid strings allowed the GA to change dominant roles as the environment changes. Those experiments focused on three scenarios where an array with twenty isotropic radiators thwarted groups of five interferers. The fist case thwarted two groups of five interferers that changed directions every twenty generations. The second scenario involved two groups of five interferers that changed every two generations, and the third scenaries focused on three groups of interferers. The first

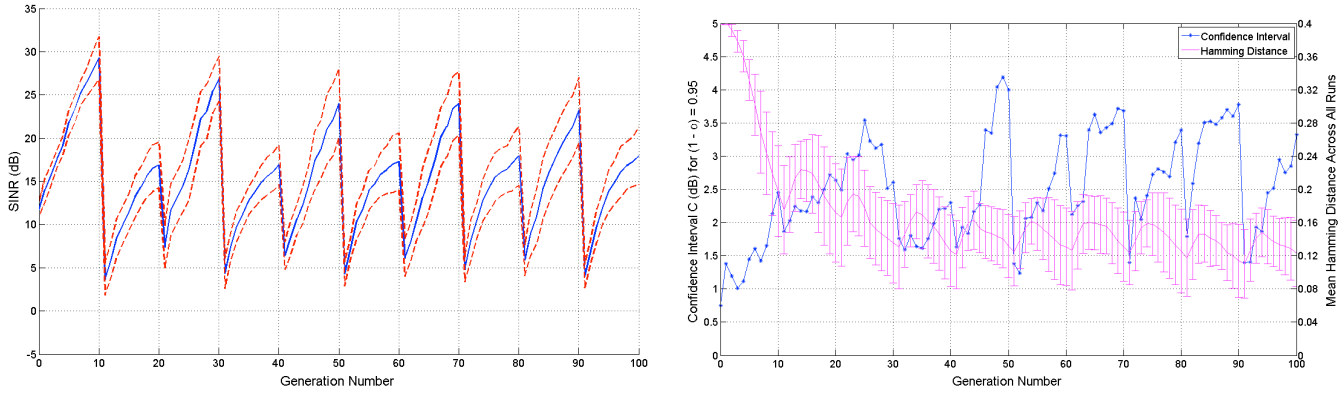

(a) (b)

Fig. 14. TDGA learning curves for stationary SOI = 0°and mobile Jammers = [45°, 200°] in first case and [120°, 300°] in second case with M = 200 strings TDGA and K = 18 runs: (a) Mean of best string SINR Fitness (dB) with ±C dB for $(1-\alpha) = 0.95$ bounds plotted, (b) Confidence interval compared to mean Hamming Distance averaged over K. Error bars represent ±1 standard deviation.

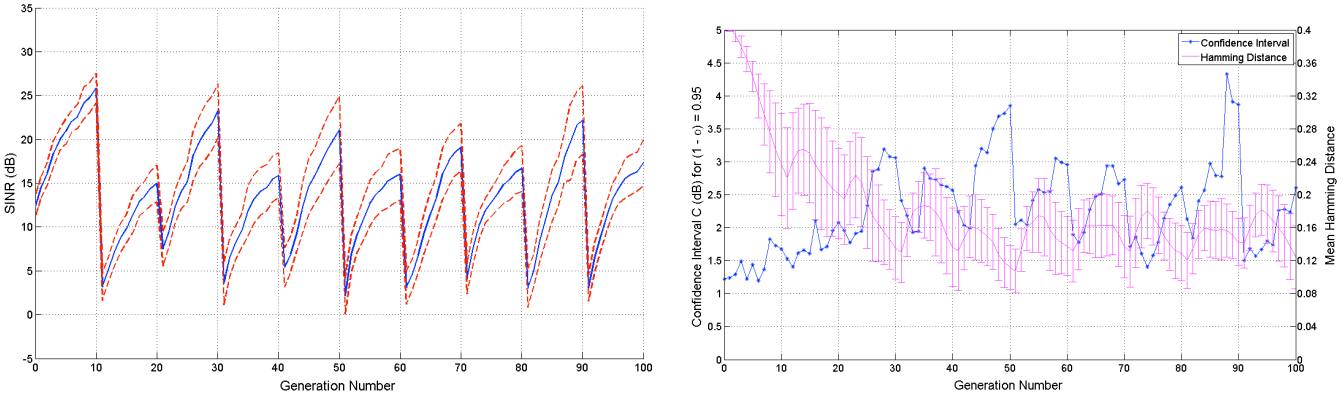

(a) (b)

Fig. 15. TDGA learning curves for mobile SOI = 0°in first case and 60°in second case and mobile Jammers = [45°, 200°] in first case and [120°, 300°] in second case with M = 200 strings TDGA and K = 15 runs: (a) Mean of best string SINR Fitness (dB) with ±C dB for $(1-\alpha) = 0.95$ bounds plotted, (b) Confidence interval compared to mean Hamming Distance averaged over K. Error bars represent ±1 standard deviation.

and third subsets radiated for 10 generations while the second subsets radiated for 20 generations [5].

The experiments presented in this paper focus on two signal sets. The first signal set has a stationary SOI at 0°, and two interferer sets: [45°, 200°] in the first case, and [120°, 300°] in the second case. The second signal set has a mobile SOI that switches between 0°and 60°. The interferer sets are the same as in the first signal set. To emulate mobility and to evaluate the TDGA's performance in adapting to mobile signals, we alternate between the two sets every 10 generations.

Fig. 14 shows the convergence results for the first signal set. Fig. 14a shows the mean of the strings having the highest SINR averaged across all K = 18 runs. The dashed lines show the confidence interval bounds with 95% confidence calculated using a Student-t distribution as described in [8]. This figure shows that the TDGA successfully adapted to a set of mobile interferers when the SOI remained stationary. The TDGA performed better with the first signal set (SOI = 0°) in general because this was the first signal set that the TDGA encountered. The confidence interval bounds are smaller for the first signal set. When the interferers changed directions, the TDGA had to relearn the search space.

Although the triallelic diploid strings allow for long term memory, it is finite and imperfect. Future work includes saving the best solutions in a memory pool for future evaluation. We will investigate other methods for preserving population diversity such as niching through fitness sharing [6].

Fig. 14b shows the confidence interval plotted with the mean Hamming Distance averaged across all K = 18 runs. They help explain the TDGA behavior shown in Fig. 14. The mean Hamming Distance is maximum at generation 0 and slowly declines. Although signal set switches at generations 10 and 20 cause brief upticks in the Hamming Distance, it continues declining until generation 30 and oscillates until the end. The confidence interval steadily increases until general 25 and declines to generation 30. After generation 30, the confidence interval oscillates in sync with the Hamming Distance.

Goldberg [6] noted that GAs can find better solutions when population diversity is high. Because the Hamming Distance is a measure of population diversity [10], our results imply that

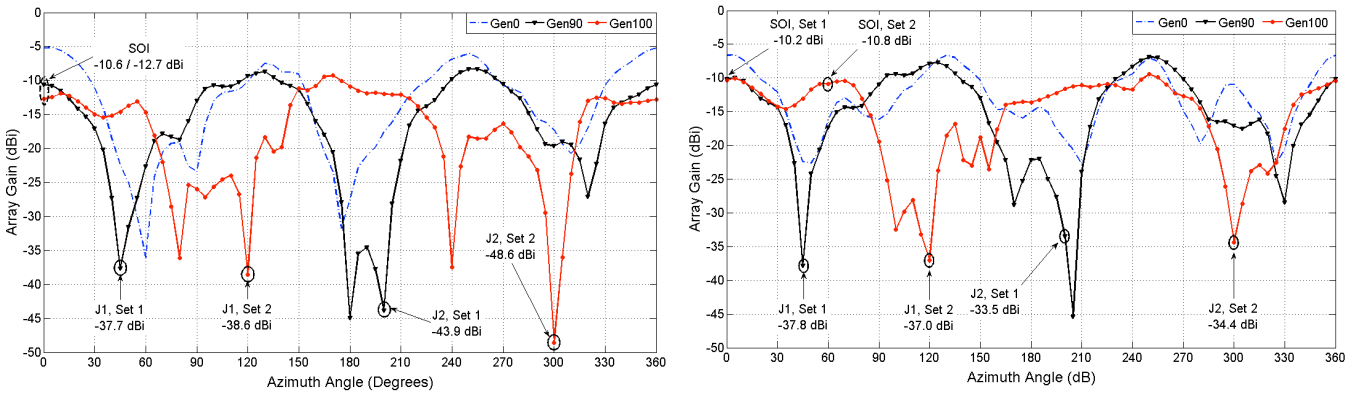

(a) (b)

Fig. 16. TDGA Azimuth radiation plots: (a) Signal Set 1: Stationary SOI = 0°and mobile Jammers = [45°, 200°] in first case & [120°, 300°] in second case, (b) Signal Set 2: All signals mobile with SOI = 0°& Jammers = [45°, 200°] in first case and SOI = 60°& Jammers = [120°, 300°] in second case.

the TDGA has a better chance on average of finding better solutions for multiple signal sets during the first few decades of each run. This does not mean that the TDGA will not find better in later generations. In individual results, the TDGA sometimes found better solutions after generation 50.

Fig. 15 shows the convergence results for the second signal set. The SOI switched between 0°and 60°while the jammers switched between [45°, 200°] and [120°, 300 °]. The results are compatible to Fig. 14. This shows that the TDGA can adapt to mobile interferers if the SOI is stationary or mobile.

Fig. 16 shows Azimuth radiation plots of best solutions found by the TDGA. Fig. 16a shows radiation plots for the first signal set. The TDGA moved the desired nulls from 45°and 200°to 120°and 300°. It sacrificed $\approx$ 2 dB of gain for the SOI while adapting to the mobile jammers.

Fig. 16b shows radiation plots for the second signal set. It directed a null at 45°with a depth of 27.6 dB below the SOI at 0°. Although the second null was off by 5°, the jammer at 200°was 22.7 dB below the second SOI at 60°. The TDGA thwarted mobile jammers when the SOI was mobile. The array gain at 60°is $\approx$ 5 dB higher compared to the same direction shown in Fig. 16a. The TDGA focused RF energy at 60°for the second signal set. As shown by Fig. 15a and Fig. 16, the TDGA would refocus nulls at appropriate locations if the SOI and jammers changed direction.

III. Conclusions

This paper showed that the SGA and TDGA were both successful in evolving an anti-jamming beamforming array in situ for 802.11b/g WiFi with results applicable to femtocells. Both versions of the GA found acceptable hardware settings to null out two stationary jammers while simultaneously focusing energy on a stationary SOI. The M = 200 strings SGA achieved best performance with the best solution having 67.8 dB SINR in convergence. The best solution that the M = 200 strings TDGA found had a 55.5 dB SINR in comparison.

However, the M = 200 strings TDGA had better statistical results. It had a final 98.7% confidence coefficient for a $\pm$3 dB confidence interval. This was significantly higher than the M = 100 strings TDGA and M = [100, 200] strings SGAs evaluated in this paper. The M = 200 TDGA also had a final 2.4 dB confidence interval with a 95% confidence coefficient assuming normality. We verified our calculations using the Student-t distribution, and the resulting confidence interval at 95% confidence was compatible with a 0.1 dB difference.

The TDGA was successful in thwarting mobile jammers regardless of the SOI's mobility. The learning curves for both signal sets were comparible. Because we did not collect 30 independent runs for the TDGA with both mobile signal sets at the time of publication, we calculated confidence intervals with 95% confidence using Student-t distribution. The confidence intervals varied in sync with the mean Hamming distances.

References

[1] J. Lohn, J. M. Becker, and D. Linden. An evolved anti-jamming adaptive beamforming network. *Genetic Programming and Evolvable Machines*, 12(3):217–234, 2011.

[2] J. Becker, J. Lohn, and D. Linden. An anti-jamming beamformer optimized using evolvable hardware. In *Proc. 2011 IEEE Intl. Conf. on Microwaves, Communications, Antennas, and Electronic Systems, IEEE COMCAS 2011*, pages 1–5, Nov. 2011.

[3] H. C. Lee, D. C. Oh, and Y. H. Lee. Coordinated user scheduling with transmit beamforming in the presence of inter-femtocell interference. In *2011 IEEE Itn'l Conference on Communications*, pages 1–5, 2011.

[4] A. Massa, M. Donelli, F. G. B. D. Natale, S. Caorsi, and A. Lommi. Planar antenna array control with genetic algorithms and adaptive array theory. *IEEE Trans. Antennas and Prop.*, 52(11):2919–2924, Nov. 2004.

[5] D. S. Weile and E. Michielssen. The control of adaptive antenna arrays with genetic algorithms using dominance and diploidy. *IEEE Trans. Antennas and Propagation*, 49(10):1424–1433, October 2001.

[6] D. E. Goldberg. *Genetic Algorithms in Search, Optimization, and Machine Learning*. Adison-Wesley, Reading, MA, 1989.

[7] J. Becker, J. D. Lohn, and D. Linden. An in-situ optimized anti-jamming beamformer for mobile signals. In *2012 IEEE International Symposium on Antennas and Propagation, IEEE APS 2012*, pages 1–2, July 2012.

[8] A. Papoulis and S. U. Pillai. *Probability, Random Variables and Stochastic Processes*. McGraw-Hill electrical and electronic engineering series. McGraw-Hill, Hoboken, NJ, Fourth edition, 2002.

[9] K. A. De Jong. *Evolutionary Computation: A Unified approach*. MIT Press, Cambridge, MA, 2006.

[10] S. Louis and G. Rawlins. Predicting convergence time for genetic algorithms. *Foundations of Genetic Algorithms*, 2:141–161, 1993.